

Strategic Planning in Topography-guided Ablation of Irregular Astigmatism After Laser Refractive Surgery

Aleksandar Stojanovic, MD; Dasa Suput, MD

ABSTRACT

PURPOSE: To identify an optimal customized ablation strategy in the treatment of eyes with secondary irregular astigmatism.

METHODS: Corneal anterior surface elevation maps of 50 eyes with secondary irregular astigmatism after decentered laser in situ keratomileusis (LASIK) or photorefractive keratectomy (PRK) and 50 virgin eyes were used for customized ablation simulations. Two ablation simulations with targeted postoperative surfaces perpendicular to either the visual or corneal morphological axis were made for each eye. All ablations were programmed for correction of corneal irregularities, including corneal astigmatism. The manifest refractive error was not corrected. Optical diameter was 6.5 mm and total diameter was 7.5 mm. Maximum ablation depths and maximum transition zone gradients were registered and analyzed.

RESULTS: In eyes with secondary irregular astigmatism, mean maximum ablation depth was $48.21 \pm 25.96 \mu\text{m}$ and $26.31 \pm 14.08 \mu\text{m}$, whereas mean maximum transition zone gradient was $29.07 \pm 25.15 \mu\text{m}$ and $9.88 \pm 6.41 \mu\text{m}$ in ablation simulations based on the visual and corneal morphological axes, respectively. The difference between the ablation strategies was highly statistically significant for both parameters ($P < .001$). In virgin eyes, only a minor difference was noted between the visual and corneal morphological axis ablation simulations ($P = .15$ for maximum ablation depths and $P = .19$ for maximum transition zone gradient).

CONCLUSIONS: In secondary irregular astigmatism, ablation based on the corneal morphological axis appears to minimize corneal tissue consumption and allows a smoother transition zone. [*J Refract Surg.* 2005;21:369-376.]

Irregular astigmatism has been one of the biggest challenges in excimer laser refractive surgery, which triggered the initial development of customized ablation in the late 1990s.¹⁻⁴ But now customized ablation's primary target has shifted towards virgin eyes.⁵⁻⁸ The published results of treatments for irregular astigmatism are not quite satisfactory,^{9,10} except for in studies by Alessio et al^{11,12} using a topography-guided system and Carones et al¹³ using a wavefront aberrometry-guided system. Current topography-guided systems are aiming to achieve a smooth aspheric cornea of a desired curvature, whereas wavefront aberrometry-guided systems aim for a flat wavefront.

The goal of this study was to identify an ablation planning strategy that spares the most tissue and where the ablated area has the smoothest transition towards the untreated cornea. The latter would assure better biologic tolerance, hence a better chance for a permanent treatment effect.¹⁴

MATERIALS AND METHODS

Corneal anterior surface elevation maps, measured by Orbscan II topographer (Bausch & Lomb, Rochester, NY), of 50 eyes with secondary irregular astigmatism after decentered myopic laser in situ keratomileusis (LASIK) or photorefractive keratectomy (PRK) (group 1) and 50 virgin eyes with regular or no astigmatism (group 2) were used for customized ablation simulations with Corneal Interactive Programmed Topographic Ablation software (CIPTA; Ligi, Taranto, Italy). The topographies in group 1 were obtained from patients referred to the Eye Department of the University Hospital of North Norway for evaluation for customized ablation retreatment of irregular astigmatism because of visual disturbances after LASIK or PRK. Patients were referred from several pri-

From the Eye Department, University Hospital of North Norway, Tromsø, Norway (Stojanovic); and the Faculty of Medicine, University of Ljubljana, Slovenia (Suput).

This study was supported by Leonardo da Vinci's Mobility Program.

The authors have no proprietary interest in the materials presented herein.

Correspondence: Aleksandar Stojanovic, MD, Fløyvn. 32, 9020 Tromsdalen, Norway. Tel: 47 90693319; Fax: 47 77647929; E-mail: aleks@online.no

Received: April 7, 2004

Accepted: November 15, 2004

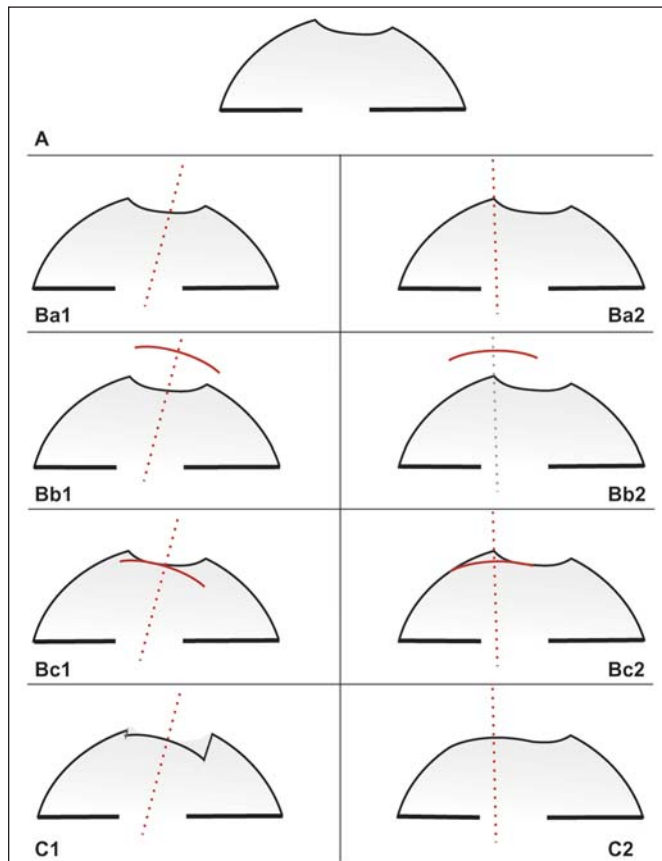


Figure 1. Schematic view of the ablation simulations. **A)** Irregular astigmatism secondary to a decentered myopic treatment before the customized ablation simulation. **Ba1, Bb1, Bc1)** Fitting of the targeted surface perpendicular to the visual axis. **Ba2, Bb2, Bc2)** Fitting of the targeted surface perpendicular to the corneal morphological axis. **C1, C2)** Simulated outcomes based on the visual and corneal morphological axes strategies.

vate clinics and other university hospitals in Norway in addition to four patients referred from abroad. The topographies in group 2 were obtained from patients seeking refractive surgery at the private SynsLaser clinic in Tromsø, Norway.

Inclusion criteria for group 1 were eyes previously treated with LASIK or PRK with decentrations >0.5 mm and postoperative astigmatism asymmetry $>\pm 3.00$ diopters (D) within a 3-mm zone. Eyes with flap or other complications after LASIK or with haze or other complications after PRK were not included. Centration of the ablation was measured as the distance between the center of the entrance pupil and the center of the ablation zone, as registered on a difference map between pre- and postoperative topography. Measurements and calculations were done according to the methodology described by Coopender et al.¹⁵ Inclusion criteria for group 2 were virgin and healthy eyes with astigmatism asymmetry of $<\pm 1.00$ D within a 3-mm zone.

ORBSCAN EXAMINATIONS

Orbscan topography is based on projection of 40 calibrated beams from two scanning slit lamps angled at 45° to the left and right of the video camera axis. Each surface point of the reflected slit beams within the central 5 mm of the cornea is independently triangulated to x, y, and z coordinates, providing true three-dimensional elevation data. To ensure a proper alignment and centration, the examiner centers the instrument axis on the corneal reflex of the fixation target while the subject fixates on the same target. In such a constellation, the corneal reflex of the fixation target represents the intercept point between the “fixation-reflex axis” and the corneal anterior surface. According to the Orbscan operating manual, the “fixation-reflex axis” is a line defined by the fixation point, its reflex on the anterior cornea of the fixating eye and the fovea. It is decided by the direction of gaze and is a member of the visual family of ocular axes, used as the primary alignment axis for all corneal topography instruments. Its intercept is readily identifiable on the topography map and was defined (for the purpose of this study) as the position of the intercept of the visual axis. The visual axis itself was identified as a line drawn through the mentioned intercept, perpendicular to the orthogonal projection of the corneal map acquired under the described conditions (axial elevation map). Accommodative status of the eye was not controlled or taken into consideration in the current study.

SIMULATIONS

An asphere with a 6.5-mm diameter was defined as the targeted surface and the center of that surface was then fit perpendicularly, first to the visual axis and second to the corneal morphological axis. Previously described “fixation-reflex axis” was defined and used in this study as the visual axis, whereas the proprietary corneal “morphological” axis is “an axis of corneal symmetry approximating the best match between the axis of the ideal shape and that of the current shape of the cornea.”¹⁶ Figure 1 shows the implication of using the two approaches.

Only correction of corneal irregularities, including corneal astigmatism, was attempted. Other ablation parameters were kept the same in all cases. An aspheric surface with basic curvature matching the flattest meridian (as registered by Orbscan topography), asphericity index (Q-value) of -0.26 , 6.5-mm optical zone, and 7.5-mm transition zone, was our targeted surface in all cases. No attempt to correct the manifest refractive error was made. Variation in pupil size was not taken into consideration.

Maximum ablation depths (in micrometers) were

TABLE 1
**Study Data for 50 Eyes with Secondary Irregular Astigmatism (Group 1)
 and 50 Virgin Eyes (Group 2)**

Group	Visual Axis		Morphological Axis	
	Mean Ablation Depth (μm)	Mean Transition Zone Gradient (μm)	Mean Ablation Depth (μm)	Mean Transition Zone Gradient (μm)
1	48.21	29.08	26.31	9.88
2	17.43	13.27	15.73	11.82

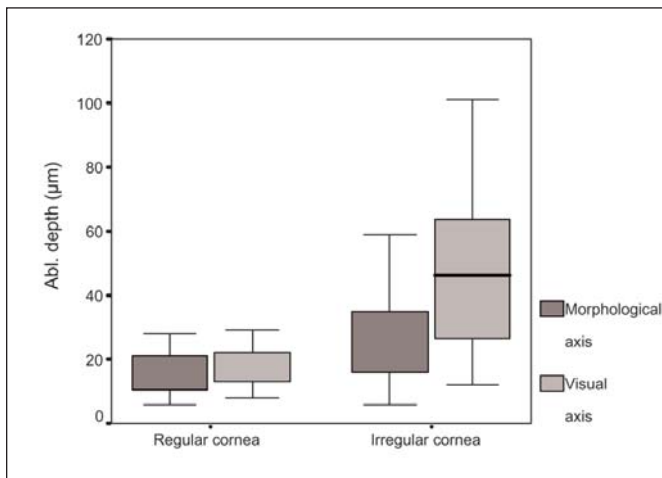


Figure 2. The difference in ablation depths between the visual and corneal morphological axes ablation simulations on regular and irregular corneas.

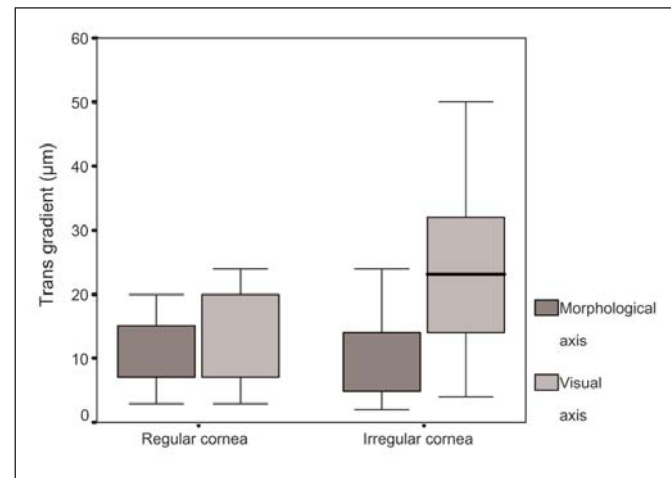


Figure 3. The difference in transition gradients between the visual and corneal morphological axes ablation simulations on regular and irregular corneas.

registered as displayed by CIPTA software. Maximum transition zone gradient (in micrometers) was obtained from the simulated treatment outcome maps by calculating the difference between the elevation at the beginning and end of the transition zone.

Results of the simulations for two treatment strategies were compared within and between the two specified groups. Two-way mixed-model analysis of variance was used in the statistical analysis.

RESULTS

Group 1 comprised topographies of 50 eyes of 50 patients with asymmetric irregular astigmatism after decentered LASIK or PRK. Mean patient age was 31.0 ± 9.1 years (range: 19 to 52 years). Thirty-six eyes were previously treated with LASIK and 14 with PRK. The mean decentration was 0.79 ± 0.26 mm (range: 0.5 to 1.5 mm) for LASIK eyes and 0.72 ± 0.21 mm (range: 0.5 to 1.4 mm) for PRK eyes. Mean astigmatism asymmetry within a 3-mm zone for group 1 was 3.66 ± 0.57 D (range: 3.1 to 5.8 D). Mean asphericity index (Q), within 4.5 mm, was $+0.21 \pm 0.62$

(range: -0.27 to $+1.87$). Group 2 comprised topographies of 50 virgin eyes of 50 patients with regular or no astigmatism with a mean age of 30.2 ± 8.7 years (range: 18 to 53 years). Mean astigmatism asymmetry within a 3-mm zone for this group was 0.78 ± 0.14 D (range: 0.5 to 0.9 D). Mean asphericity index (Q), within 4.5 mm, was -0.24 ± 0.11 (range: -0.49 to 0.22).

Mean maximum ablation depth and mean maximum transition zone gradient for both ablation strategies for both groups are presented in Table 1. The difference between the two treatment strategies in group 1 was highly statistically significant for both parameters ($P < .001$). In group 2, only a minor difference was noted between the visual and morphological axis ablation simulations ($P = .15$ for maximum ablation depths and $P = .19$ for maximum transition zone gradient) (Figs 2 and 3).

DISCUSSION

The principal elements of the optical system of the eye (cornea, pupil, and crystalline lens) are not cen-

tered with respect to each other. Additionally, the eye's neural (visual axis and the line of sight) and optical (geometrical) axes do not coincide because of the eccentric placement of fovea. Consequently, the target object can be placed on fovea only by rotation of the eye, making the eye a decentered optical system. Hence the eye, and specifically the corneal optics, can be considered and analyzed from a geometrical (morphological) and neural (visual) aspect.

The definition of the visual axis used in the current study is somewhat different from the commonly used definition where the visual axis is described as a line connecting the fixation target and fovea through nodal points.¹⁷ Nevertheless, both axes belong to the family of visual axes, and in our opinion, either is well-suited for the purpose of demonstration of how customized ablation based on data that reflect the rotational position of a fixating eye works. The problem of defining the visual axis from corneal topography only emphasizes the difficulties in considering geometrical and visual optics of the eye at the same time. The interpretation of axial maps (axial elevation map and axial curvature map), which are by definition orthogonal to the visual axis, is especially problematic in eyes with decentered corneal optics, where the visual axis tends to be volatile.

Ablation planning in excimer laser corneal refractive surgery has traditionally been based on measurements that in one way or another reflect the eye's visual function. Wavefront aberrometry, autorefractometry, Placido-based corneal topography, and even manifest refraction are all dependent on patient's fixation during the examination. Consequently, the data or maps acquired under such circumstances are referenced to the rotational position of the fixating eye. The concept of using the measurements that reflect the eye's visual function seems logical in refractive surgical ablation planning, as the goal of the refractive surgery is improvement of the existing visual function. Such a concept has also proved to be successful in standard and customized excimer laser treatments of virgin eyes. Unfortunately, the same reasoning cannot be applied to the treatment of cases with visual disturbances secondary to induced asymmetric corneal irregularities after refractive surgery, other eye surgery, corneal injuries, etc. Decentered corneal optics radically change the eye's visual optics, forcing the visual axis to move from its original (physiologic) position to a new one, as the eye adapts to the changed optical circumstances by assuming a new rotational position to place the targeted image on the fovea. An ablation plan that uses topography or aberrometry information referenced to the visual axis (or line of sight) would attempt to op-

imize the corneal optics on the basis of a pathological rotational position. Additionally, the dependence of the visual axis on the accommodative status further emphasizes its instability and makes it even less suitable for customized ablation planning.

Patients with secondary irregular astigmatism are subject to visual disturbances that often lead to serious disabilities. They need treatment, but often have a very limited amount of corneal tissue. The ablation depth is therefore of primary concern in this patient category. The other factor of major concern is the transition smoothness towards the untreated cornea, which determines whether the ablated area would remain as planned or be filled with epithelium or changed after it is covered by a LASIK flap. The current study investigated the influence of centration and orientation of ablation profile on simulated outcomes of customized treatments of secondary irregular astigmatism after decentered ablations. Investigated parameters were limited to the amount of tissue removal and the smoothness of transition zone because of the availability of these parameters for direct measurement as well as of their importance in retreatments for this particular patient category. Other factors that would reflect the quality of the ablation plans, such as results of Zernike or Fourier analysis of the simulated postoperative corneal surface, might provide additional answers, whereas a clinical study provides the possibility of analysis of the visual outcomes, biological tolerance of the actual ablations, and their biomechanical effects.

Although the material from the current study comprised only the cases of secondary irregular astigmatism after LASIK or PRK, our conclusions are most probably applicable to secondary irregular astigmatism with any other etiology, as the decentration of corneal optics, a key feature in all cases of secondary irregular astigmatism, was the decisive factor regarding evaluation of the customized ablation strategy.

Several published studies describe customized ablation treatments for irregular astigmatism⁹⁻¹³ but none discuss the ablation planning alternatives. The main point of this study is to show that three-dimensional global assessment of the corneal shape and evaluation of alternative treatment should be a part of customized ablation planning for secondary irregular astigmatism. The impact of this seems to be increasing with the amount of preoperative corneal asymmetry.

Among the topographies from the current study, five cases had decentered myopic treatments (decentration 1.2 to 1.5 mm), resulting in significant secondary irregular astigmatism. For these cases, retreatment simulations based on the visual axis resulted in the maximum transition gradient being greater than the

TABLE 2
Previously Treated Corneas With Decentrations

Patient	Visual Axis		Morphological Axis	
	Ablation Depth (μm)	Transition Zone Gradient (μm)	Ablation Depth (μm)	Transition Zone Gradient (μm)
1	53	96	23	14
2	59	100	34	14
3	46	100	21	28
4	64	90	30	20
5	69	90	39	20

maximum ablation depth. Most of the ablation was applied to the area that had already been treated by the primary surgery (that caused the decentration), further increasing the height difference between the treated and untreated cornea. On the other hand, the simulations based on corneal morphological axis in the same five corneas placed the majority of the ablation on the most elevated (previously untouched) area and showed much smoother transitions and shallower ablations (Table 2). Figures 4, 5, and 6 show three-dimensional views of patient 1 (see Table 2); a preoperative view, as well as the views of postoperative simulations based on visual and corneal morphological axis. It seems that the treatment simulations based on the corneal morphological axis attempted to “recenter” the primary treatment by placing the ablation on the previously untreated area, which should have been treated during the primary surgery, whereas the treatment simulations based on the visual axis attempted to optimize the primary decentered treatment area, increasing the corneal asymmetry.

By the nature of their design, wavefront aberrometers measure the optical properties of the whole eye and are aligned coaxially with the eye’s line-of-sight (defined as the line passing through the center of the eye’s entrance and exit pupils connecting the object of regard to the foveola).¹⁸ The wavefront aberrometry-guided customized ablation systems do not consider any direct information from the corneal surface. For compiling their ablation patterns, these systems currently use an asphere with a curvature of $R=7.78$ mm and an average asphericity of -0.3 as their reference surface, from which the measured wavefront aberrations are subtracted.¹⁹ That reference surface is by definition perpendicular to the line-of-sight, which also belongs to the family of visual axes. The concept takes a “local” approach and uses wavefront data con-

structed around the line of sight, without considering any information from beyond the ablation area. In secondary irregular astigmatism, this can result in an ablation that further increases the corneal asymmetry and causes an abrupt transition towards the untreated area, as in the cases from the current study where the targeted surface was fit to the visual axis (see Table 2). Klein²⁰ recognized the problem of deep ablation when treating a dominant coma with wavefront-guided customized ablation, and he suggested introduction of a small amount of tilt of the reference plane to reduce the ablation depth. Nevertheless, without registering the corneal morphology and spatial pachymetry and estimating the effect of an ablation on the cornea, the risk of not detecting a potentially dangerous situation is imminent. We therefore suggest that ablation map calculated by wavefront-guided systems should always be correlated with corneal elevation and pachymetry map before treatment of cases with major corneal asymmetry.

In addition to ablation planning, a three-dimensional corneal surface assessment would also help recognize the direct effect of the cause of secondary irregular astigmatism (decentered ablations, scarring after corneal injuries, keratitis, etc) locally as well as its influence on the global corneal morphology that might occur due to the secondary corneal biomechanical response.²¹ Currently, only the corneal elevation topography would allow a three-dimensional assessment of the corneal surface and evaluation of a variety of treatment options.

To our knowledge, only the CIPTA customized ablation software “freely” explores the ablation possibilities because it is able to uncouple itself from the visual axis perspective. It can “take a global look” at the raw elevation data and consider the corneal shape from a purely morphological aspect. This opens a possibility for a free three-dimensional floating of the desired

Customized Ablation for Irregular Astigmatism/Stojanovic & Suput

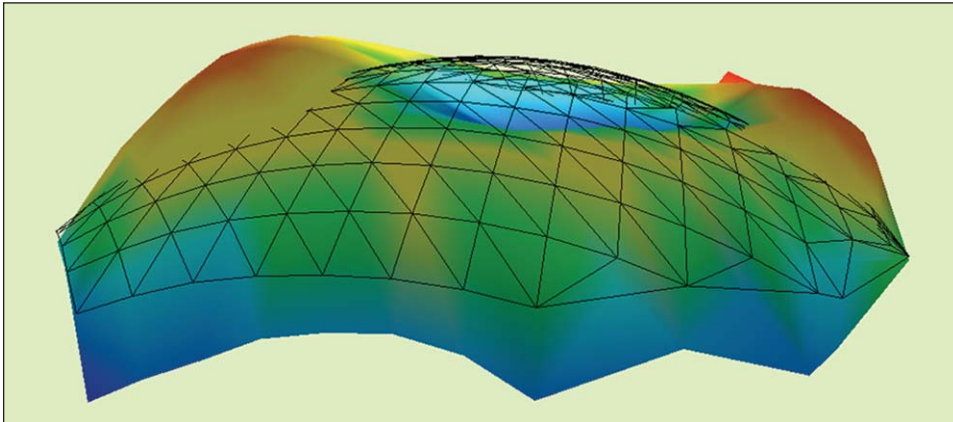


Figure 4. Patient 1. Three-dimensional view of the irregular astigmatism secondary to a decentered myopic treatment before the customized ablation simulation.

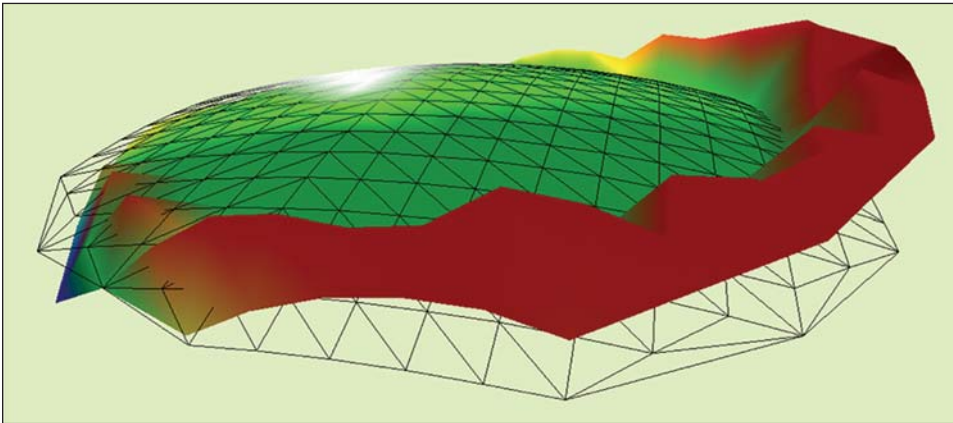


Figure 5. Patient 1. Three-dimensional view of the simulated outcome based on the visual axis strategy showing a high transition gradient between the treated and untreated area.

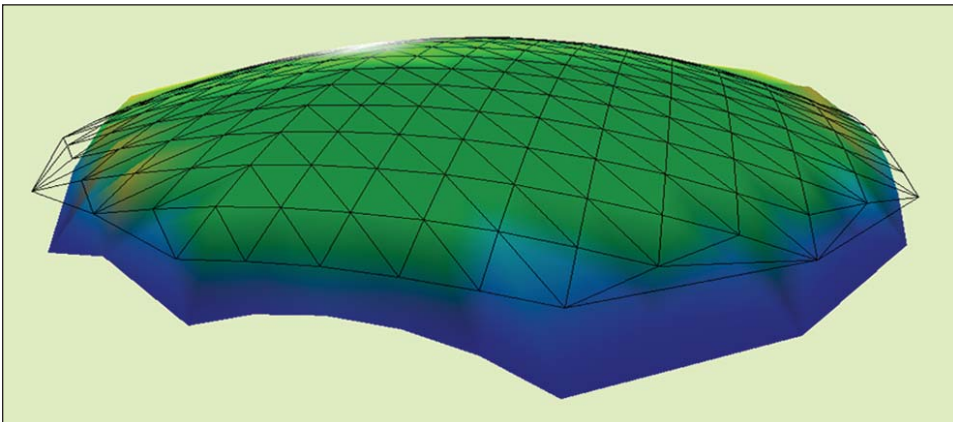


Figure 6. Patient 1. Three-dimensional view of the simulated outcome based on the corneal morphological axis strategy showing a smooth transition gradient between the treated and untreated area.

targeted surface providing infinitely more ablation alternatives than the systems referenced to visual axis. AstraPro customized ablation system (LaserSight, Orlando, Fla) bases its ablation planning on the corneal elevation data referenced to the visual axis and places its targeted surface perpendicular to that axis. Such an approach results in deep ablations in cases with secondary irregular astigmatism, and the AstraPro provides a solution to that problem by using so-called “advanced” ablation planning alternative. In that case, the software automatically adjusts the ablation center (but keeps the ablation axis orientation unchanged) until

the targeted surface is fit to a position that requires the least amount of tissue removal. T-cat customized ablation system (WaveLight Laser Technologie, Erlangen, Germany) uses Placido disk-based topography information. Curvature data (referenced to the visual axis) are converted to elevation data and decomposed into orthogonal Zernike polynomials. Because this approach, which is similar to the AstraPro and visual axis strategy of CIPTA, results in too deep ablations in treatments of secondary irregular astigmatism, T-cat provides an ablation planning alternative where the tilt component can be removed from the ablation plan.

This way the orientation of the fitting axis is changed to a new position that results in reduced tissue removal, but the centering of the ablation axis is kept intact, ie, still attached to the intercept of the visual axis. In their default constellation, both AstraPro and T-cat systems base their ablation on the same axis on which the topographic measurements were acquired, ie, the visual axis. They obviously recognize the problem of that approach in treatment of secondary irregular astigmatism and they allow for modifications of either centration or orientation of the visual axis, but none of the two systems leaves it completely. On the other hand, the CIPTA system is able (in its morphological axis mode) to completely uncouple itself from the visual axis and consider the corneal morphology without a bias.

Ablation plans from the current study based on the corneal morphological axis strategy showed a significant advantage in simulated treatments of secondary irregular astigmatism with respect to ablation depth and transition smoothness; nevertheless, because this strategy disregards the visual axis, the postoperative corneal surface might not be perpendicular to the postoperative visual axis, causing a prismatic effect with an uncertain visual implication. Unfortunately, the same can happen in treatments using the visual axis strategy, because the poorly defined and unstable visual axis in eyes with secondary irregular astigmatism would most probably change its position after the surgery. Hence it seems as though certain misalignment is unavoidable in any case, unless we can identify the position of the original (virgin) visual axis and plan the ablation of the secondary irregular astigmatism accordingly. However, it seems that the potentially negative effect of the tilt of the postoperative corneal surface relative to visual axis is not visually significant and that it should be acceptable weighed against the patient's preoperative visual disturbances that are being addressed with the treatment. Mrochen et al²² claim that the eye's ability to rotate would easily compensate for such a tilt; however, the amount of tilt tolerated by the eye is still unknown. We could add that the binocular function after the treatment, which none of the available systems consider, will be a decisive factor in evaluating the tolerance of the prismatic effect after the surgery.

Concerning virgin eyes with regular corneas, the current study showed that ablation plans compiled on the corneal morphological and visual axes did not differ much in ablation depth or transition smoothness. This implies that the concept of using the measurements referenced to visual axis (or line of sight) is a good solution in the treatment of virgin eyes, and the current results of the customized ablations⁵⁻⁸ seem to support this.

Concerning secondary irregular astigmatism, the placement and axis of the simulated customized ablations differed significantly for the two strategies. Morphological axis strategy attempts to restore "damaged" optical symmetry of the cornea, whereas the visual axis strategy attempts to optimize the visual optics of the aberrated eye. The latter strategy may result in dangerously deep ablation in previously thinned areas, as shown in the current study. Therefore, systems that have given excellent results in customized ablation of virgin eyes generally cannot be used for treatment of secondary irregular astigmatism.

REFERENCES

1. Seitz B, Langenbacher A, Kus MM, Harrer M. Experimental correction of irregular corneal astigmatism using topography-based flying-spot-mode excimer laser photoablation. *Am J Ophthalmol.* 1998;125:252-256.
2. Wiesinger-Jendritza B, Knorz MC, Hugger P, Liermann A. Laser in situ keratomileusis assisted by corneal topography. *J Cataract Refract Surg.* 1998;24:166-174.
3. Dausch D, Schroder E, Dausch S. Topography-controlled excimer laser photorefractive keratectomy. *J Refract Surg.* 2000;16:13-22.
4. Alessio G, Boscia F, La Tegola MG, Sborgia C. Topography-driven photorefractive keratectomy: results of corneal interactive programmed topographic ablation software. *Ophthalmology.* 2000;107:1578-1587.
5. Lawless MA, Hodge C, Rogers CM, Sutton GL. Laser in situ keratomileusis with Alcon CustomCornea. *J Refract Surg.* 2003;19: S691-S696.
6. Cosar CB, Saltuk G, Sener AB. Wavefront-guided laser in situ keratomileusis with the Bausch & Lomb Zyoptix System. *J Refract Surg.* 2004;20:35-39.
7. Vongthongsri A, Phusitphoykai N, Nariphthapan P. Comparison of wavefront-guided customized ablation vs. conventional ablation in laser in situ keratomileusis. *J Refract Surg.* 2002;18: S332-S335.
8. Dausch D, Dausch S, Schroder E. Wavefront-supported photorefractive keratectomy: 12-month follow-up. *J Refract Surg.* 2003;19:405-411.
9. Alio JL, Belda JI, Osman AA, Shalaby AM. Topography-guided laser in situ keratomileusis (TOPOLINK) to correct irregular astigmatism after previous refractive surgery. *J Refract Surg.* 2003;19:516-527.
10. Hjortdal JØ, Ehlers N. Treatment of post-keratoplasty astigmatism by topography supported customized laser ablation. *Acta Ophthalmol Scand.* 2001;79:376-380.
11. Alessio G, Boscia F, La Tegola MG, Sborgia C. Topography-driven excimer laser for the retreatment of decentralized myopic photorefractive keratectomy. *Ophthalmology.* 2001;108:1695-1703.
12. Alessio G, Boscia F, La Tegola MG, Sborgia C. Corneal interactive programmed topographic ablation customized keratectomy for correction of postkeratoplasty astigmatism. *Ophthalmology.* 2001;108:2029-2037.
13. Carones F, Vigo L, Scandola E. Wavefront-guided treatment of abnormal eyes using the LADARVision platform. *J Refract Surg.* 2003;19:S703-S708.
14. MacRae S, Schwiegerling J, Snyder RW. Customized and low spherical aberration corneal ablation design. *J Refract Surg.* 1999;15:S246-S248.

Customized Ablation for Irregular Astigmatism/Stojanovic & Suput

15. Coopender SJ, Klyce SD, McDonald MB, Doubrava MW, Kim CK, Tan AL, Srivannaboon S. Corneal topography of small-beam tracking excimer laser photorefractive keratectomy. *J Cataract Refract Surg.* 1999;25:674-684.
16. Alessio G, La Tegola MG, Sborgia C. Corneal interactive programmed topographic ablation using the lasersight laser. In: MacRae SM, Krueger RR, Applegate RA, eds. *Customized Corneal Ablation.* Thorofare, NJ: SLACK Inc; 2001:261-269.
17. Pande M, Hillman JS. Optical zone centration in keratorefractive surgery: entrance pupil center, visual axis, coaxially sighted corneal reflex, or geometric corneal center? *Ophthalmology.* 1993;100:1230-1237.
18. Thibos LN, Applegate RA, Schwiegerling JT, Webb R, VISA Standard Taskforce Members. Standard for reporting the optical aberrations of eyes. In: MacRae SM, Krueger RR, Applegate RA, eds. *Customized Corneal Ablation.* Thorofare, NJ: SLACK Inc; 2001:348-361.
19. Mrochen M, Jankov M, Bueeler M, Seiler T. Correlation between corneal and total wavefront aberrations in myopic eyes. *J Refract Surg.* 2003;19:104-112.
20. Klein SA. Optimal corneal ablation for eyes with arbitrary Hartmann-Shack aberrations. *J Opt Soc Am A Opt Image Sci Vis.* 1998;15:2580-2588.
21. Roberts C. The cornea is not a piece of plastic. *J Refract Surg.* 2000;16:407-413.
22. Mrochen M, Krueger RR, Bueeler M, Seiler T. Aberration-sensing and wavefront-guided laser in situ keratomileusis: management of decentered ablation. *J Refract Surg.* 2002;18:418-429.